

Compaction of Single Supercoiled DNA Molecules Adsorbed onto Amino Mica

L. A. Limanskaya^a and A. P. Limanskii^{a, b, 1}

^a Mechnikov Institute of Microbiology and Immunology, Academy of Medical Sciences of Ukraine, ul. Pushkinskaya 14/16, Kharkov, 61057 Ukraine

^b Laboratory of Plasma Membrane and Nuclear Signaling, Graduate School of Biostudies, Kyoto University, Kyoto, 606-8502 Japan

Received December 16, 2005; in final form, March 24, 2006

Abstract—A model of possible conformational transitions of supercoiled DNA in vitro in the absence of proteins under the conditions of increasing degree of compaction was developed. A 3993-bp pGEMEX supercoiled DNA immobilized on various substrates (freshly cleaved mica, standard amino mica, and modified amino mica with a hydrophobicity higher than that of standard amino mica) was visualized by atomic force microscopy in air. On the modified amino mica, which has an increased density of surface positive charges, single molecules with an extremely high degree of compaction were visualized in addition to plectonemic DNA molecules. As the degree of DNA supercoiling increased, the length of the first-order superhelical axis of molecules decreased from 570 to 370 nm, followed by the formation of second- and third-order superhelical axes about 280 and 140 nm long, respectively. The compaction of molecules ends with the formation of minitoroids about 50 nm in diameter and molecules of spherical shape. It was shown that the compaction of single supercoiled DNA molecules immobilized on amino mica to the level of minitoroids and spheroids is due to the shielding of mutually repulsing negatively charged phosphate groups of DNA by positively charged amino groups of the amino mica, which has a high charge density of its surface.

Key words: amino mica, atomic force microscopy (AFM), DNA compaction, supercoiled DNA, toroid

DOI: 10.1134/S1068162006050074

INTRODUCTION

The genomic DNA of giant length (from millimeter to meter) in bacterial nucleoids and eukaryotic nuclei whose volume is from as little as a few to hundreds cubic micrometers is compacted to higher ordered structures by interactions with proteins and other compounds [1].² In its turn, the volume of, e.g., *E. coli* nucleoid constitutes only about one fourth of the cell volume. In the absence of proteins, a randomly compacted DNA molecule occupies a much greater volume than in the nucleus or nucleoid of a bacterial cell. According to modern views, the compaction of DNA in eukaryotic cells is due to its interaction with a number of proteins, first of all, topoisomerases and histones, followed by the formation of nucleosomes, chromatin fibers, and chromosomes [2–4]. In this process, histones neutralize in vivo up to 57% of negatively charged phosphate groups of DNA [5], and the remaining charge is neutralized by other positively charged

ions of the cell environment, including mono- and multivalent cations, which constitute up to 1% of cell mass [6].

About ten histone-like prokaryotic proteins that participate in DNA compaction are known. The DNA-binding proteins HU (heat unstable) and H-NS (histone-like nucleoid structuring) are among them; they exhibit no specificity to the DNA nucleotide sequence [7]. Other proteins show specificity to DNA sequence upon binding; these are IHF (integration host factor) and HMG (high-mobility group) proteins modulating the histone binding to DNA. In addition, condensins and cohesins that belong to the SMS group (structural maintenance of chromosome) were identified, which play a key role in the condensation of chromosomes and lead to direct condensation of DNA [8].

The structural organization of genome in the nucleus of eukaryotes is studied using various model systems. It was found by AFM that the structure of the *E. coli* nucleoid changes during the cell growth: in the stationary phase it is more compact than in the log phase. However, in both phases, stationary and log, the nucleoid is formed by fibers of about 80 nm diameter [1]. In addition to the 80-nm fiber, a finer fiber of 40-nm

¹ Corresponding author; phone: (38)-057 7001-708; fax: (38)-057 7003-410; e-mail: o.lymunskiy@mail.ru.

² Abbreviations: AFM, atomic force microscopy; APTES, 3-aminopropyltriethoxysilane; scDNA, supercoiled DNA; overscDNA, supercoiled-coil DNA.

diameter and a highly ordered loop were visualized in the log phase of the nucleoid development.

Another model system, nucleosome, which is the main repeating unit of chromatin, also received a wide recognition. In this case, structures like “beads-on-string” were visualized for linearized DNA in the complex with a histone octamer formed by two molecules of each of the proteins H2A, H2B, H3, and H4 [9]. The compaction and condensation of DNA with the formation of toroids and fibers (rod-like structures) can also be achieved under the conditions other than complexation with proteins [10, 11]. Numerous studies showed that polycations (polylysine, protamine, cobalt hexamine) and natural (spermine⁴⁺, spermidine³⁺) and synthetic polyamines (diaminopropane²⁺) can cause the DNA condensation and the formation of toroids [12–15]. Moreover, it was demonstrated that the presence of proteins and water-soluble multivalent cations is not necessary for the DNA condensation [16]. The condensation of DNA followed by AFM visualization can also be accomplished by immobilizing its molecules on the positively charged surface of amino mica (as opposed to the variant with the use of freshly cleaved mica in the presence of metal cations, due to the limitations inherent in this method). The degree of DNA condensation can thus be varied by applying aminosilane derivatives used for a modification of mica and by changing the NaCl concentration during DNA immobilization [16, 17]. However, the use of a narrow range of NaCl concentrations (10–100 mM) in the works permitted no obtaining of highly compacted DNA structures other than toroids. Interestingly, under the conditions of condensation of linear DNA molecules, multimolecular aggregates rather than condensed structures from single DNA molecules were formed [18, 19].

Thus, the compaction of DNA to the level of nanoparticles is a fundamental biological phenomenon that plays an important role in the DNA packing in viruses, prokaryotic nucleoids, eukaryotic nuclei, and in the development of nonviral systems for the transport of genetic information to eukaryotic cells *in vitro* and *in vivo* (using cationic liposomes and polypeptides for DNA condensation) [16].

In this study, we obtained images of single scDNA molecules whose degree of compaction far exceeds that achieved previously. The use of a new substrate for DNA immobilization, we had previously developed, which is a modified amino mica with a higher density of positive surface charges and a higher hydrophobicity [20] as compared with the standard amino mica, enabled the visualization of successive stages of compaction of single circular DNA molecules. Compacted structures were detected that are formed both by a two-fold and fourfold decrease in the length of the superhelical axis of molecules with the subsequent formation of rod-like structures and second- and third-order superhelical axes, respectively, and by the subsequent assembly of single scDNA molecules into minitoroids,

semispheroids, and spheroids with the formation of oversupercoiled structures (overscDNA).

RESULTS AND DISCUSSION

The surface of mica, a standard substrate for AFM, is negatively charged in buffer solutions at neutral pH values [21]. Therefore, the immobilization of negatively charged DNA molecules on the mica surface is carried out using several approaches that enable a change in the total negative surface charge of mica to the positive [9, 22, 23]. Note that the surface of freshly cleaved (i.e., unmodified) mica has hydrophilic properties, which is expressed in the spreading of a drop of a DNA solution on the mica surface. At the same time, amino mica obtained by the modification of mica with aminosilanes [23], which carry positively charged amino groups on their surface, has clearly observed hydrophobic properties, which is visually manifested in the fact that a DNA drop does not spread on the surface but takes the shape close to spherical [20]. Mica can be modified by aminosilanes in both solution (in this case, self-associated monolayers of aminosilane molecules are formed on the surface of amino mica) [24, 25] and in gas phase [22]. In the first variant, the adsorbed DNA molecules are at a distance of about 1 nm from the mica surface (with the use of APTES) [24]. In the second variant, which is used in this study, this distance is much more difficult to determine, because the structure of the surface layer of amino mica has been studied only by indirect methods. For example, an analysis of AFM images of structures such as spheroids and dimers compacted on the amino mica obtained in gas phase indicates that scDNA molecules appear to be partially immersed into the surface layers of aminosilane. Adjacent to these structures with an increased density are always regions of amino mica in which the height of the aminosilane layer is substantially less than its height in the absence of spheroids or dimers [26, 27].

The localization of DNA molecules immobilized on the surface of amino mica radically differs from that on freshly cleaved mica (in the presence of Mg²⁺). In the first case, DNA molecules are at a much greater distance from the mica surface than upon adsorption onto mica coated with magnesium ions. In addition, the “dip” of a DNA molecule in aminosilane layers on the mica surface provides, due to volume interactions, not only a stronger (compared with linear interactions in the case of freshly cleaved mica in the presence of Mg²⁺) shielding of negatively charged phosphate groups of DNA by positively charged amino groups exposed on the amino mica surface, but also a dynamic mobility of DNA molecules.

The substrates for DNA immobilization used in this study can be arranged in the order of increasing hydrophobicity as follows:

freshly cleaved mica < standard amino mica < modified amino mica.

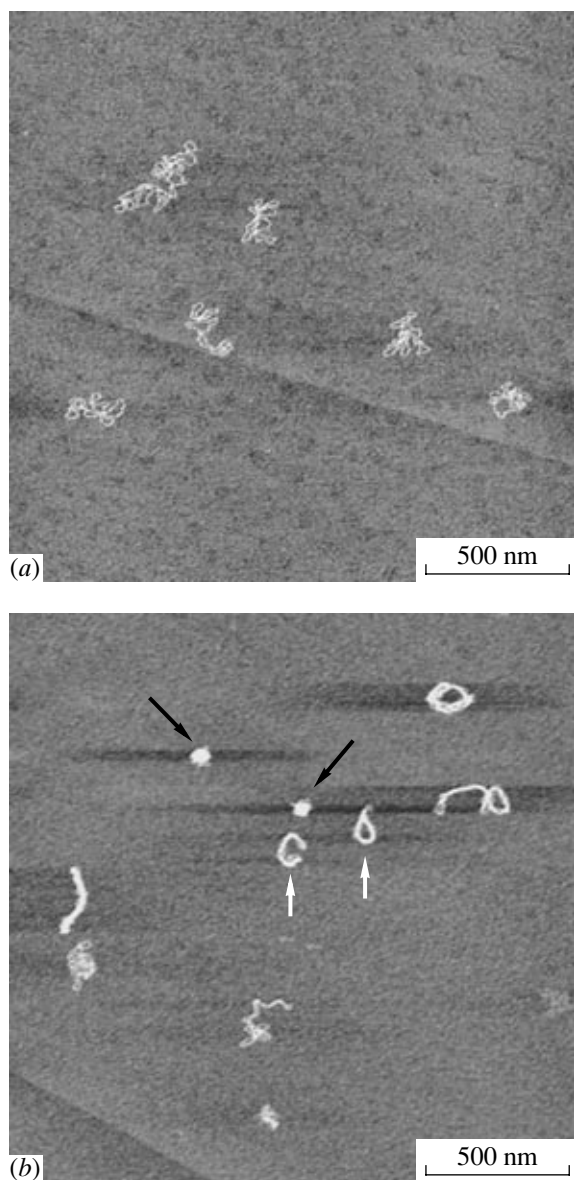


Fig. 1. AFM image of supercoiled pGEMEX DNA in air after the application of DNA solution in TE buffer on the surface of (a) **standard amino mica** and (b) **modified amino mica**. Supercoiled DNA molecules of different degrees of compaction, from (a) plectonemic to (b) supercoiled-coil molecules with different lengths of the superhelical axes (two molecules in toroidal conformation and in a conformation close to toroidal, are shown by white vertical arrows) and DNA in spheroidal conformation (two spheroids are shown with inclined black arrows) are presented. The scan size for both images is $2\ \mu\text{m} \times 2\ \mu\text{m}$.

The immobilization of scDNAs on the modified amino mica, which has a higher density of positive surface charges [26, 27] compared not only with freshly cleaved mica but also with the standard amino mica [26, 27], leads to a substantial compaction of DNA molecules (Fig. 1). The table gives the most typical variants for 98 visualized single overcDNAs with the corresponding parameters out of 108 individual scDNA

molecules (the remaining ten molecules are the intermediate variants of condensed molecules shown). The amount of plectonemic scDNAs (A2) with a low density of supercoils (with σ of approximately -0.024) is 21%; overcDNAs with a high value of σ of about -0.13 , which form the first-order superhelical axis (B3), amount to 12%; overcDNAs forming the second-order superhelical axis (C3, B2, C2) amount to 27%; molecules forming the third-order superhelical axis (D2, D3, E2) amount to 14%; and the most compacted molecules, spheroids, constitute 17%.

The physicochemical properties of amino mica obtained by modification in vapors of aminosilane derivatives and used as a substrate for AFM have insufficiently been studied. Only rough estimates of the surface density of amino groups were obtained. For example, it was found for the standard amino mica that only 50% of amino groups exposed on the surface are active, i.e., protonated (the information for the modified amino mica is unavailable). However, based on the measurements of the half-period of activity (the time during which the amount of immobilized DNA molecules decreases two times) of standard and modified amino mica (by calculating the amount of immobilized DNA molecules on a certain area of amino mica after its storage in argon atmosphere) [26], we presume that almost all amino groups of the modified amino mica are protonated.

Despite a great number of experimental studies of the DNA interaction with multivalent cations, the theoretical aspects of this phenomenon were investigated insufficiently. Even small polyamines cannot be represented as simple point ions, as assumed in classical theories of polyelectrolytes, e.g., in the condensation theory of Manning [29] and the Poisson–Boltzmann theory [30]. The Manning condensation theory, which predicts the direct relationship between the neutralization of DNA charge and the concentration of mono- and multivalent ions and which was preferred in the 1970–1980s, states that about 90% negative charge of phosphate groups should be neutralized for DNA compaction [15]. However, the experiments carried out by integral methods (e.g., by calorimetric analysis) indicated that DNA condensation proceeds at different degrees of neutralization of the charge of DNA phosphate groups, from 67% for cobalt hexamine to 87% for spermidine [31]. In addition, it was shown that the theoretical approach of Manning is a rather rough approximation of the Poisson–Boltzmann theory [32]. Therefore, M. Frank-Kamenetskii proposed to revise the conclusions of the Manning theory or take them with caution [32].

The consideration of DNA as an infinitely long negatively charged cylinder (in terms of the maximally simplified model of the theory of polyelectrolytes), one negative charge was determined to be located on an area of $1.07\ \text{nm}^2$ [33]. At the same time, a dodecylammonium cation can occupy an area of $0.90\ \text{nm}^2$, which points out, in the opinion of the authors of [33], that the

Parameters of pGEMEX scDNA molecules (contour length, volume, and others) determined from AFM images. The excluded volume for pGEMEX DNA (3993 bp) $V = 4010 \text{ nm}^3$












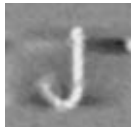
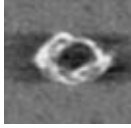
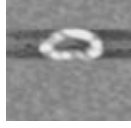
Variant in Fig. 6*	Molecule(s)	Maximum height H_{\max} , nm	Minimal height h_{\min} , nm	Contour length of a supercoiled molecule l , nm	Length of superhelical axis l , nm	Volume of molecule V , nm^3
A3 ^d (3)		0.80	0.35**	1243	466 ^a	3510
A2 ^e (21)		0.99	0.35**	1216	–	3530
B3 (12)		0.95	0.35**	567	567 ^a	4440
C3 (16)		1.69	0.78	279	279 ^b	3280
B2 (4)		1.35	0.28**	260	260 ^b	3470
C2 (7)		1.36	0.30**	270	270 ^b	3520
D2 (3)		3.00	1.25	140	140 ^c	5180
D3 (7)		1.74	0.84	260	260	3980
E2 (4)		2.60	1.85	–	–	3620
E3 (17)		3.45	0.30**	–	–	3140
B1 (1)		1.40	0.35**	548	548	6300

Table (Contd.)

Variant in Fig. 6*	Molecule(s)	Maximum height H_{\max} , nm	Minimal height h_{\min} , nm	Contour length of a supercoiled molecule l , nm	Length of superhelical axis l , nm	Volume of molecule V , nm ³
E1 (1)		2.00	0.87	269	269 ^c	7080
C1 (1)		2.00	0.45**	–	401	6840
D1 (1)		2.10	0.30**	267	267	6570

* The number of molecules visualized for each variant is given in parentheses.

** Double-stranded DNA.

^a Length of the first-order superhelical axis; ^b Length of the second-order superhelical axis; ^c Length of the third-order superhelical axis;

^d DNA is adsorbed on unmodified mica; ^e DNA is adsorbed on standard amino mica.

DNA charge could be completely neutralized during the DNA–cation interaction.

Recent calculations of DNA–counterion interactions by the method of molecular dynamics yielded unexpected results. For example, it was reported in [34] that there are fundamental differences in the interaction of DNA with natural (spermidine³⁺ and spermine⁴⁺) and synthetic (diaminopropane²⁺) polyamines. First, it was shown that the binding of NH₃⁺ or Na⁺ cations to one site on the DNA practically rules out the binding of another cation to the adjacent site located at a distance of less than 0.8 nm, due to electrostatic repulsion. In other words, the binding sites for the polycations studied are localized along the double-stranded DNA at a distance of 0.4 nm from each other, whereas the adjacent binding sites for the cations were estimated in [33] to be separated by a distance of 0.17 nm along the axis. Second, it was demonstrated that, unlike the natural polyamines, a synthetic diaminopropane polycation can form bridges between the adjacent phosphate groups along the DNA chain.

We estimated the density of amino groups on the silicon surface, which, to a first approximation, can be considered as similar to the surface of mica after treatment with APTES. In the first variant, in which one APTES molecule reacts with three OH groups exposed on the silicon surface (according to the model of the APTES-treated surface [35]), one amino group was localized on the area of 12.90 nm². At the same time, it was experimentally found for the surface of silicon nitride (material used for manufacturing AFM probes [36]) that the number of amino groups on an area of 1 × 10⁶ nm² after modification with APTES in the gas phase is 1730 ± 200 [35], which corresponds to one amino

group on an area of 6 × 10² nm². In the second variant, at the presumption that one APTES molecule reacts with one OH group of the oxidized silicon surface, we found that one NH₂ group is localized on the area of 3.87 nm². These estimates are consistent in the order of magnitude with the conclusions in [34] from which we calculated that the binding site for the cation on DNA occupies an area of 2.51 nm². In this case, at the cation binding sites distance of 0.4 nm along the DNA strand, 42% negative charges of phosphate groups would be neutralized in the reaction with polycations provided that all binding sites on DNA are occupied with polycations.

Thus, these data indicate that the interaction of DNA with the surface of modified amino mica is qualitatively similar to the DNA–polyamine interactions of DNA molecules with the positively charged matrix whose hydrophobicity varies depending on the procedure of mica modification in gas phase.

Also note that the surface properties of amino mica are determined by a variety of factors. For example, it was empirically established that the standard amino mica used as an AFM substrate for DNA visualization can be obtained by the treatment in the vapors of only distilled APTES in an atmosphere of inert gas. The use of undistilled APTES (which undergoes hydrolysis in an atmosphere of air) leads to amino mica with a low surface charge density, which is unsuitable for obtaining high-quality DNA images [20].

The surface properties of amino mica (elasticity and charge) can be characterized by various methods, including X-ray spectroscopy and AFM force measurements, by means of the determination of the amount of

protonated amino groups and the adhesion force, respectively. Using AFM force measurements for standard amino mica, we have previously determined the adhesion force (i.e., the force necessary for separating the surfaces of amino mica and the probe that come and remain in contact during approaching) to be about 2–4.6 nN in TE buffer for various probes [36]. On the other hand, it has been established that the topology of scDNA immobilized on amino mica is just the most sensitive peculiar indicator of the suitability of amino mica surface, since amino mica is used as a substrate for the visualization of linear and scDNAs.

Single scDNA molecules forming the second-order superhelical axes are shown in Fig. 2a. The lengths of the superhelical axes of these highly compacted molecules decreased, compared with plectonemic DNA, to one fifth of the contour length of the relaxed molecule ($l = 260$ nm).

Another variant of the highly compacted scDNA molecule formed on the surface of modified amino mica is a spheroid (Fig. 2a). For a more precise calculation of the volume, we as a rule used the longitudinal section of the molecule by a secant plane perpendicular to the plane of mica rather than the height of an overscDNA molecule measured at one point (which substantially varies): with a characteristic height of the double helix of DNA immobilized on mica of 0.3–0.4 nm, the height at the nodes formed by two twisted DNA strands may be as much as 1.3–1.8 nm.

It is possible to obtain the number of compacted supercoiled DNA molecules involved in the formation of a particular aggregate from the volume of the condensed structure calculated directly from the AFM image. The DNA volume is easily calculated by multiplying the DNA diameter by the area of the cross section of the molecule upon the assumption of the B-form of DNA (i.e., the distance between the bases along the axis of the double helix $h = 0.34$ nm). For example, the volume of spheroid V calculated from the area of the cross section and the diameter given in Fig. 2a is 3140 nm³. Since the excluded volume of the pGEMEX DNA under the assumption of the B-form DNA is $V_{\text{excl}} = 4010$ nm³, these results suggest that the spheroid is formed by a single DNA molecule.

Further compaction results in the formation of molecules with even twofold lesser length of the superhelical axis (the length of the third-order axis $l = 140$ nm, variant D2, table) and molecules of spherical conformation, such as semispheroids (variant E2, table) and spheroids (E3, table).

The compaction on the modified amino mica occurs not only in the case of single DNA molecules. Figure 2b presents an image of a dimer ($V 7080$ nm³), a compacted structure formed by two DNA molecules; the length of the superhelical axis of the dimer is 260 nm as is the length of the superhelical axis of a single molecule (Fig. 2a).

Compacted Molecules are Formed not Only by Dimers but also by Single DNA Molecules

The condensation of DNA by the action of various factors, including proteins [10, 11], has earlier been demonstrated only for dimers and trimers, but not for single DNA molecules. Therefore, let us consider in detail the S-shaped overscDNA molecule shown in Fig. 2a, which is in a conformation similar to toroidal. The AFM image of this molecule at a higher-resolution (Fig. 3a) and its three-dimensional image (Fig. 3b) clearly demonstrate that it is formed by several distinct strands (a part of the molecule formed by three locally diverging strands is shown by arrows in Fig. 3a). From the profile of the section (Fig. 3b) drawn through these strands (the line along which the secant plane was drawn perpendicular to the plane of the figure is shown in the insert), it is possible to determine the height of these strands. Note that a possibility to measure the height of a biopolymer immobilized on the substrate at a subnanometer resolution (!) is an extremely important feature of AFM, which favorably distinguishes it from electron microscopy also in this respect. Since the height of two DNA strands is 0.3 nm and the height of the third strand is 0.6 nm, this means that two separated scDNA strands are double-stranded DNAs and the strand whose height is equal to the doubled height of the DNA molecule on mica ($h 0.6$ nm) is formed by two twisted double-chain strands.

Thus, an analysis of this section profile indicated that the S-shaped overscDNA is formed by four double-chain DNA strands. The contour length of the overscDNA is 260 nm, and one can conclude that this compact structure is formed by a single circular DNA molecule “folded in two”. Note that, with a contour length l of 260 nm, the number of DNA strands in the section profile for a dimer should be equal to eight.

Another section profile of this C-shaped molecule is shown in Fig. 3d, which confirms that it is formed by strands whose heights are equal to the height of the double-stranded DNA ($h 0.3$ nm). In fact, the analysis of the section profile, along with the determination of the excluded volume of the molecule, also enables to differentiate monomolecular structures from the aggregates formed by several molecules. A thorough analysis of AFM images of overscDNA (e.g., Figs. 3a and 3d) indicates that the height of two twisted DNA strands forming the scDNA is equal to twice the height of a strand of the double-stranded DNA ($h 0.3$ nm) provided only that the strands are wrapped around each other and are tight against one another. Otherwise, when the strands are twisted relative to one another but do not closely adjoin each other, the height of the molecule may be as great as 1.3–1.8 nm.

We visualized one more structure, a minitoroid, which is superficially similar to the spheroid on the low-resolution AFM image. Figure 4 shows a minitoroid formed by a single scDNA, the section profiles, and the three-dimensional image of the molecule. The vol-

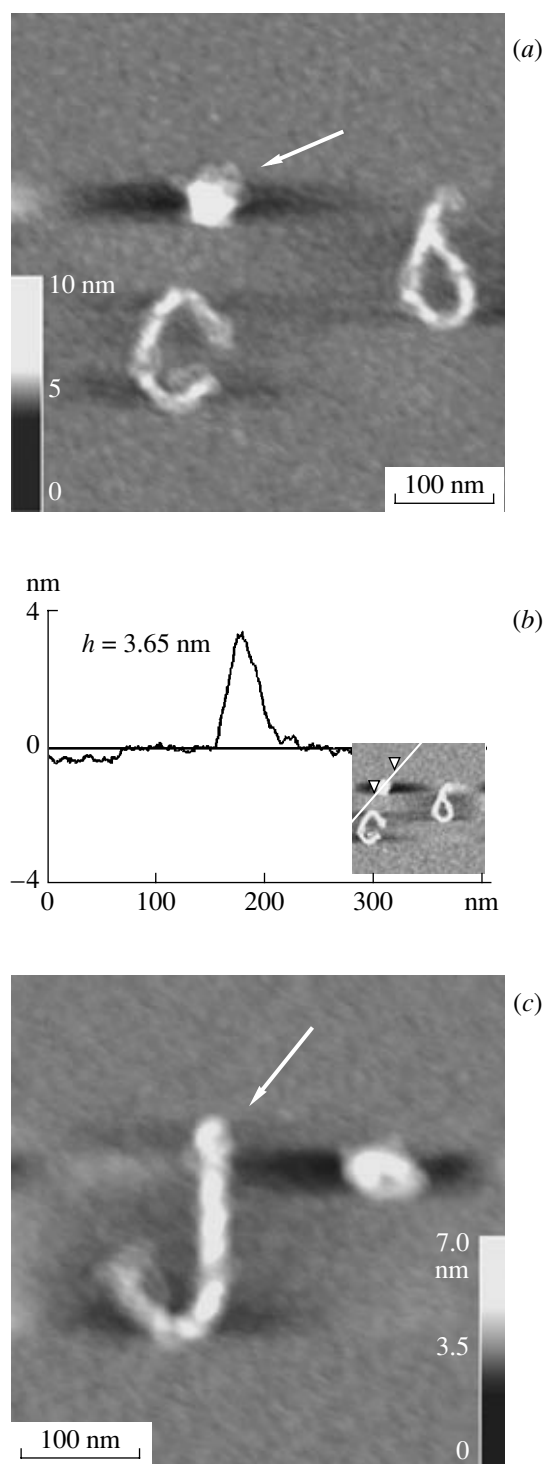


Fig. 2. AFM image of single pGEMEX scdDNA molecules, their dimers, and spheroids on modified amino mica. (a) The length of the second-order superhelical axis of each of the DNA molecules is 260–270 nm, i.e., about one fourth of the contour length of the relaxed molecule. The arrow shows a spheroid. The gray shading scale corresponding to the 0–10 nm range of the Z coordinate is given, which enables one to determine the height of the immobilized molecule. The scan size is 500 nm × 500 nm. (b) Section profile of the DNA molecule in spherical conformation, which makes it possible to determine the height of the molecule. The maximal height of the spheroid $h_{\max} = 3.65$ nm. The line along which the section was made is shown in the insert. (c) AFM image of a dimer formed by two over-scDNA molecules (shown by an arrow) with the length of superhelical axis of 260 nm and the volume equal to the doubled volume of a single scDNA molecule. The scan size is 500 nm × 500 nm. The gray shading scale corresponds to the 0–10 nm range of Z coordinate. Near the dimer, a semispheroid formed by a single DNA molecule is adsorbed.

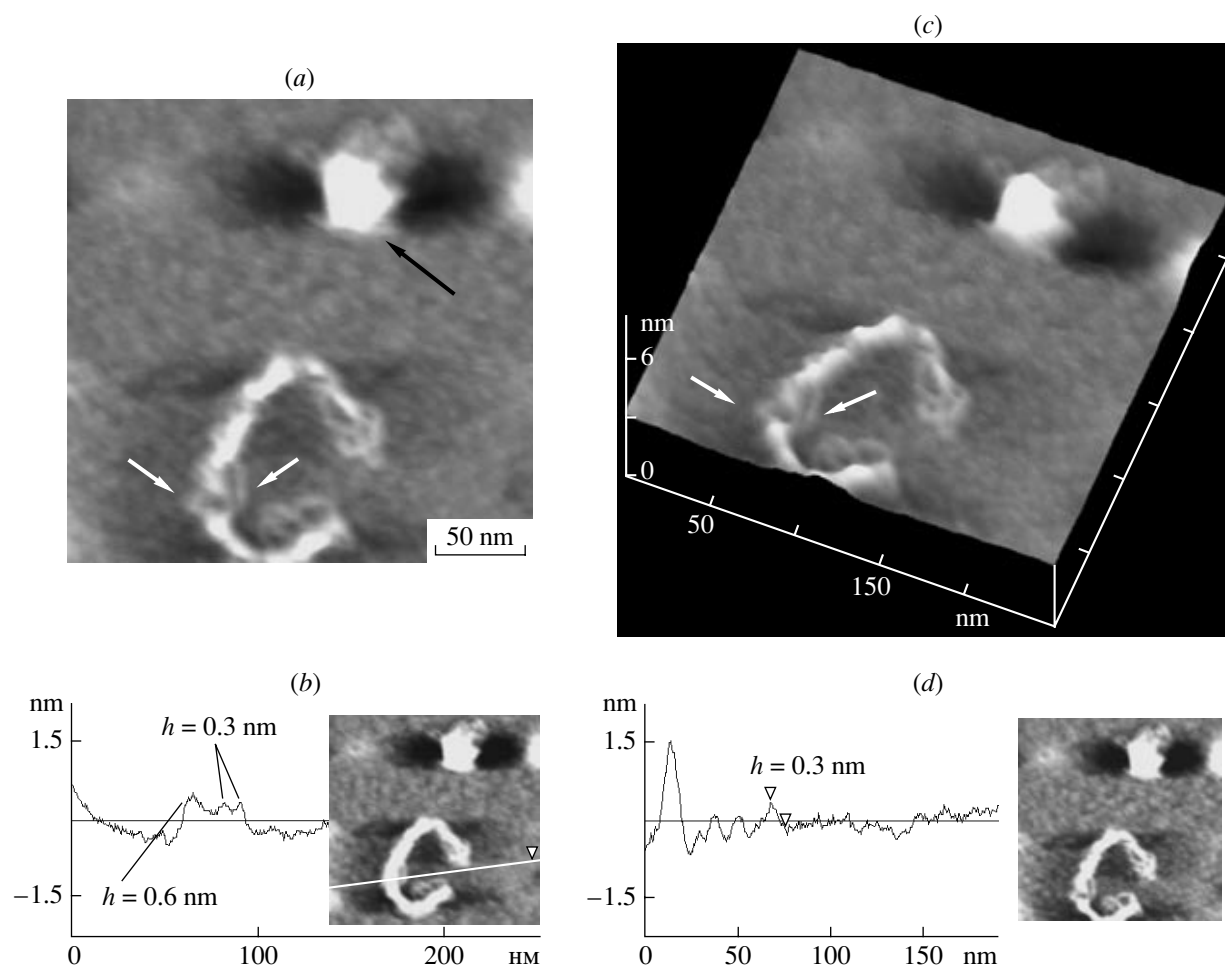


Fig. 3. (a) AFM image, (b, d) section profiles, and (c) a three-dimensional image of a single pGEMEX over-scDNA molecule that forms the second-order helical axis. (a) Arrows show separated DNA strands whose section profile is shown in Fig. 4b. The black arrow shows a spheroid. (b) The line along which the secant through three separated strands is drawn is shown in the insert. The height of two peaks is 0.3 nm, and the height of the third peak is 0.6 nm. (d) The profile of the section drawn through the separated strands of over-scDNA; the secant plane is drawn along the line shown in the insert. The height of these strands is 0.3 nm, which corresponds to the height of the strand of the double-strand DNA. The scan size is 250 nm \times 250 nm.

ume of this molecule is 3980 nm³, which corresponds to the volume of a single pGEMEX DNA molecule. One can see from the section profiles in Figs. 4b and 4c that three of four segments of the toroid have the equal heights (h 1.74 nm), whereas the fourth segment is almost twice as little in height (0.84 nm). This means that the fourth segment has the number of turns of the scDNA rod-like structure less than in the other three segments; i.e., the minitoroid is a peculiar minitoroid with a slit in the upper part whose length is equal to one quarter of the circumference length.

The parameters of the majority of visualized compacted scDNAs are given in the table. It has earlier been shown that several linear or circular DNA molecules are involved in the formation of toroids [12, 16, 19, 37]. We also visualized toroids formed by two over-scDNAs. In all positions of the table, except for the dimeric rod of variant E1, the characteristics of AFM images of single DNA molecules are given.

Compaction of over-scDNA Molecules Occurs with the Formation of Second- and Third-Order Superhelical Axes

It has earlier been established that the length of the scDNA axis remains constant within the superhelix density range of $0.03 < |\sigma| < 0.12$ and constitutes about 35% of the contour length of a relaxed molecule [38]. This condition is fulfilled for the pGEMEX scDNA molecules adsorbed onto freshly cleaved mica, which has a relatively low surface charge density. In this case (Fig. 5a), the length of the superhelical axis is 466 ± 5 nm (which is 35% of the contour length of DNA under the assumption of its B form), the superhelix density $\sigma = -0.024$, and the number of nodes $n = 7-8$. For scDNA immobilized on the surface of modified amino mica, molecules with both a much higher superhelix density and different lengths of superhelical axes were visualized (Figs. 5b–5d). The length of the superhelical axis of the molecule shown in Fig. 5b is 567 ± 18 nm,

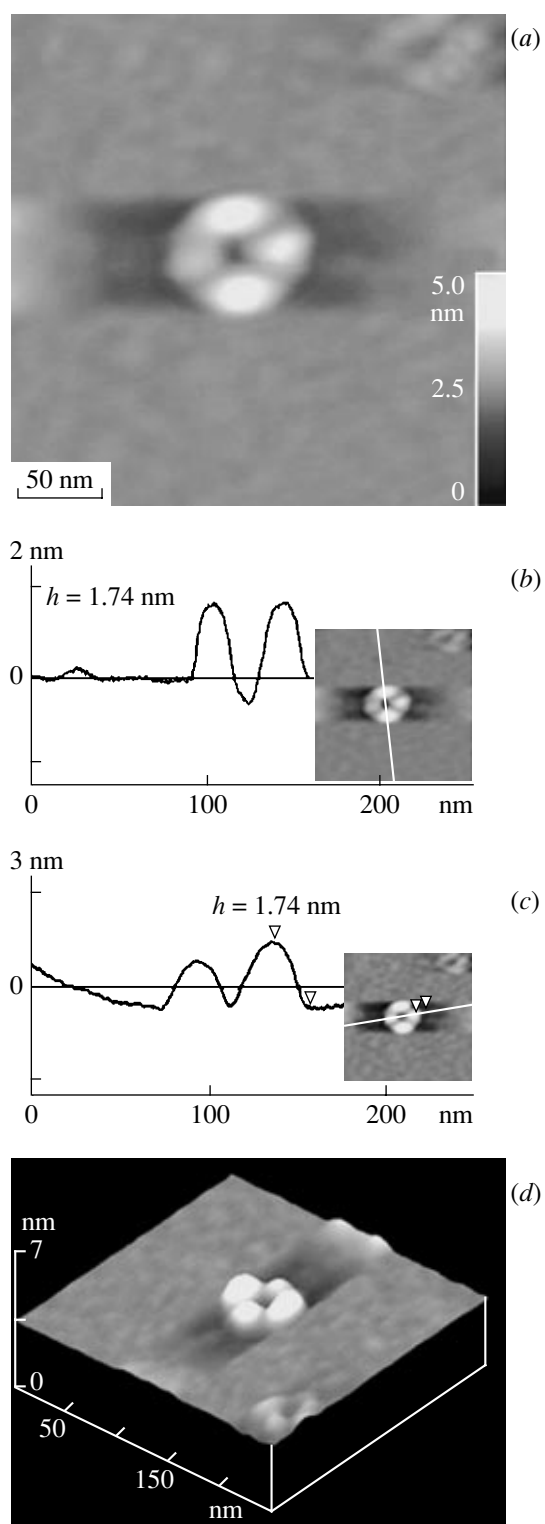


Fig. 4. (a) AFM image, (b, c) section profiles, and (d) a three-dimensional image of a single pGEMEX overscDNA molecule that forms a minitoroid. (a) The scan size is $250 \text{ nm} \times 250 \text{ nm}$. (b) The height of two toroid segments through which the secant plane is drawn is 1.74 nm . (c) The heights of two other toroid segments, which were determined from the section profile, are 1.74 and 0.84 nm , respectively. The secant planes are drawn along the lines shown in the inserts. Triangles show the corresponding peak on the section profile and the level relative to which the height of the large peak was measured. The height of this segment of the minitoroid is 1.74 nm . (a, d) The external diameter of the minitoroid is $50\text{--}60 \text{ nm}$, and the internal diameter is $15\text{--}25 \text{ nm}$.

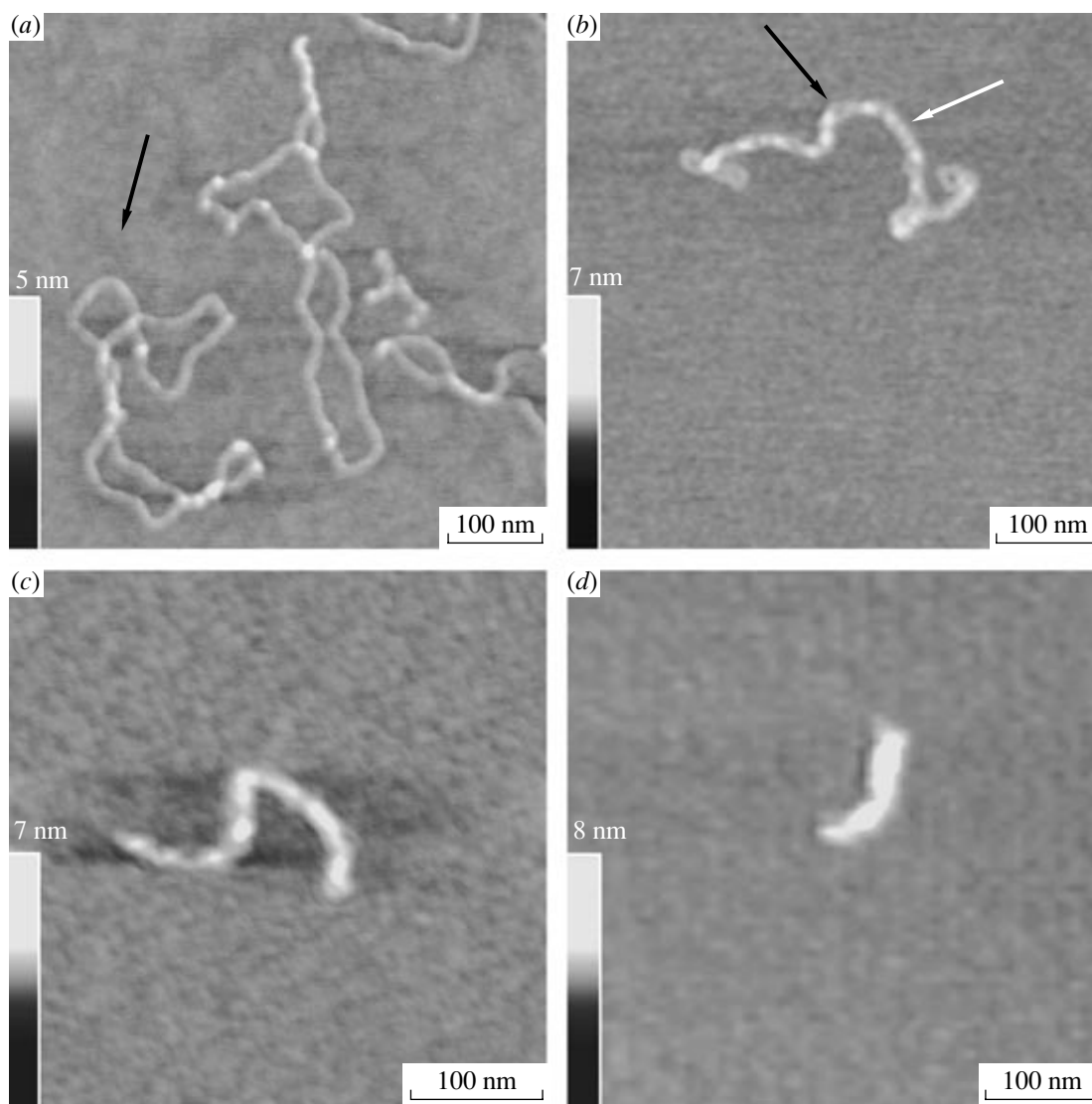


Fig. 5. AFM image of pGEMEX scDNA with different lengths of the superhelical axes. DNA is immobilized on (a) a freshly cleaved mica from a buffer containing Mg^{2+} and (b–d) on modified amino mica. (a) The length of the superhelical axes are 466 ± 5 nm for both molecules. The molecule shown by an arrow has seven nodes or mutual intersections of DNA strands and is characterized by a superhelix density σ of -0.024 . (b) l is 567 nm, σ -0.13 ; the molecule has 19 nodes. DNA fragments for which the profiles of cross and longitudinal sections shown in Fig. 7 were plotted are indicated by black and white arrows, respectively. (c) overscDNA with the second-order superhelical axis of 279 nm and the number of nodes equal to seven. (d) overscDNA with the third-order superhelical axis of 140 nm. The upper limits of the gray shading scale corresponding to the height of the object on the image are (a) – 5, (b, c) – 7, and (d) – 8 nm. (a–d) The length of the segment corresponds to 100 nm.

but the number of nodes ($n = 19$) is considerably greater, and the superhelix density σ is -0.13 .

We also visualized DNA molecules with considerably smaller lengths of superhelical axes, $l = 279$ nm (Fig. 6c) and 140 nm (Fig. 5d) upon the immobilization on the surface of modified amino mica. Since the volumes of both molecules correspond to that of a single pGEMEX DNA molecule, it can be assumed that the molecule with l of 279 nm (Fig. 5c) is formed as a result of folding in two of the molecule with l of 567 nm (Fig. 5b), and the molecule with l of 140 nm (Fig. 5d), as a result of folding in two of the molecule with l of

279 nm (Fig. 5c). Thus, upon immobilization of scDNA molecules on the surface of amino mica with a rather high density of amino groups, we visualized overscDNAs forming the second-order (Fig. 5c) and third-order superhelical axes (Fig. 5d) whose lengths are, respectively, about two and four times less than the length of the first-order superhelical axis (Fig. 5b).

Based on the analysis of the AFM images obtained, we proposed a scheme of step-by-step compaction for both single DNA molecules and dimers (Fig. 6). Variants B1, C1, D1, and E1 designated by rectangles correspond to scDNA dimers, which was determined by

tonemic DNA molecules but are more compact, i.e., are localized on a smaller area of the substrate.

Several variants of scDNA compaction can be seen upon going to modified amino mica (all other images were obtained with it), which is characterized by a much higher surface charge density and a higher hydrophobicity than standard amino mica. At the first stage, the number of nodes increases, and over-scDNAs (B3) with the length of the superhelical axis equal to about half the contour length of the relaxed molecule are formed, which resemble peculiar rods in the appearance.

At the second stage, this rod-like molecule is folded in two, the length of the superhelical axis further decreases two times and is about one fifth of the contour length of the relaxed molecule (C3, B2, C2). At this stage, both further formation of rod-like structures (C3) and the formation of toroids (C2) can occur. At the third stage, shorter rods (D2) with even twice as little length of the superhelical axis, $l \sim 140$ nm, are formed. In addition, a minitoroid (D3) can be formed from both toroid (C2) and a rod-like molecule (C3). At the fourth stage, the further compaction of toroids and rods leads to the formation of semispheroids (E2) and spheroids.

High-resolution AFM images of these highly compacted DNA molecules are presented in Fig. 7. Interestingly, these minitoroids appear both as groups (Fig. 7a) and as single structures (Fig. 4a).

An attempt to answer the question why different DNA molecules are compacted to a different degree leads to the assumptions that (i) protonated amino groups are nonuniformly immobilized on the surface of modified amino mica and (ii) spheroids and semispheroids are formed in the regions of modified amino mica that have a maximal density of reactive amino groups. The localization of morphologically similar forms of scDNAs (minitoroids and rod-like molecules with the lengths of superhelical axes of 570 and 280 nm) on the mica sites of about 500×500 nm suggests that the densities of the surface charges of the modified amino mica vary. The presence of this charge density gradient just leads to different degrees of shielding of the DNA phosphate groups and, as a consequence, to the formation of morphologically different variants of compacted scDNAs. In addition, a DNA sample under study contains a set of topoisomers that have different supercoil densities. In the case when the characteristic time of DNA compaction is comparable with the access time of DNA molecules to the amino mica surface, topoisomers with different numbers of supercoils can condense to aggregates with different compaction degrees.

Another compaction variant is the scDNA compaction of dimers rather than single molecules. The molecules whose AFM images are shown in positions B1, C1, D1, and E1 form dimers, as determined from their calculated volumes. Two plectonemic molecules (A1

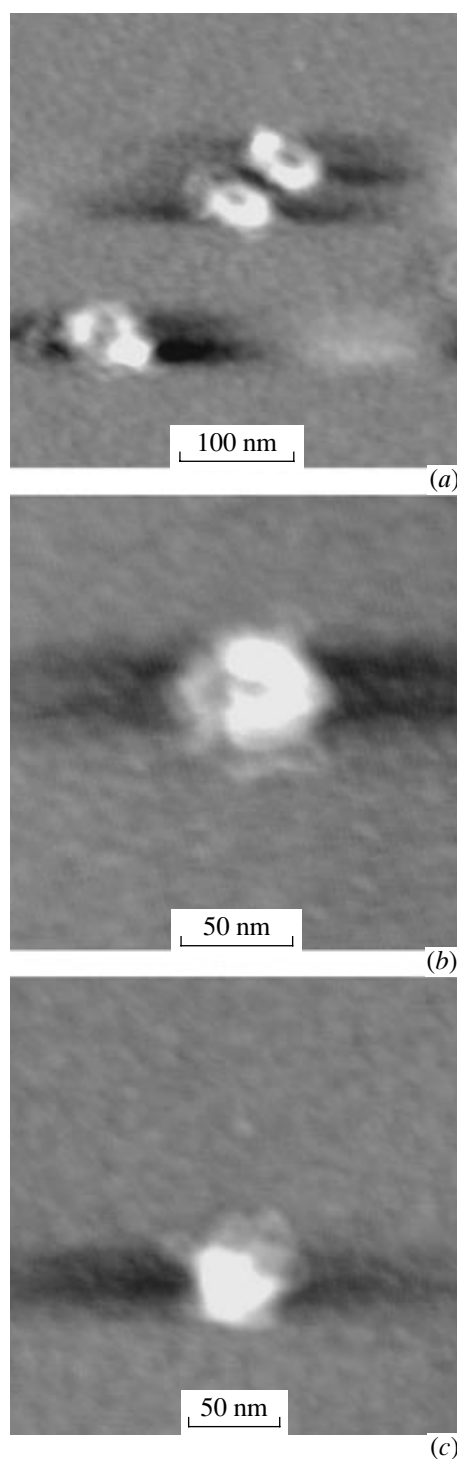


Fig. 7. AFM images of compacted molecules of pGEMEX scDNA. (a) Three minitoroids formed by single DNA molecules. The scan size is $400 \text{ nm} \times 400 \text{ nm}$. (b) Semispheroid with a height in a maximum h_{max} 2.6 nm. The height of the uncompacted DNA strand is 0.3 nm, which corresponds to the height of double-stranded DNA. The scan size is $250 \text{ nm} \times 250 \text{ nm}$. (c) Spheroid with a height h_{max} 3.45 nm. The scan size is $250 \text{ nm} \times 250 \text{ nm}$.

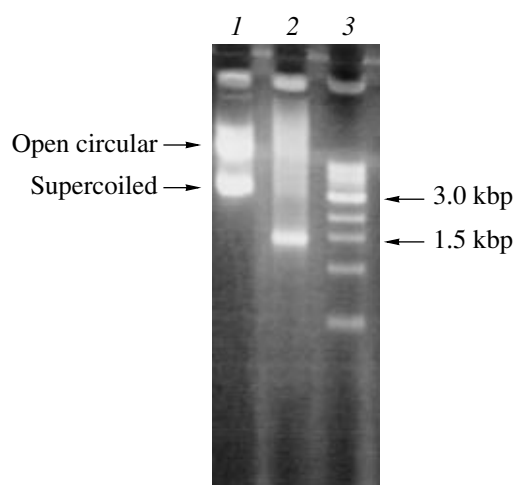


Fig. 8. Analysis of pGEMEX1 scDNA after electrophoresis in 2% agarose gel followed by staining with ethidium bromide. Lane 1, pGEMEX1 scDNA with the expected length of 3993 bp; 2, a 1400-bp amplicon; 3, a 1000-bp marker. The 3000-bp marker stands out due to its higher intensity.

and A2) initially form rod-like structures (B1). Then a toroid (C1 and D1) or a rod (E1) with the superhelical axis length being one fifth of the contour length of the relaxed molecule can be formed. Position D2 also corresponds to a toroid formed by two overscDNA molecules.

Thus, we proposed the model of DNA compaction. It shows that, at a high surface charge density of the substrate on which DNA molecules are immobilized, the compaction of not only dimers and trimers of DNA but also of single DNA molecules can occur. The use of modified amino mica with a high surface charge density results in an extremely high compaction of single scDNA molecules (along with the compaction of dimers) due to the shielding of negatively charged phosphate groups of DNA by positively charged protonated amino groups of modified amino mica.

As distinct from the earlier studied multimolecular compaction of linearized and scDNA molecules, we investigated the compaction of single scDNA molecules. As the density of DNA supercoils increases, a decrease in the length of the superhelical axis takes place (remember that, according to earlier studies, the length of the superhelical axis remains unchanged as the density of supercoils increases and constitutes just 35% of the contour length of the relaxed molecule [38]). Further compaction of single DNA molecules is first characterized by the formation of the second-order helical axis (the length of the superhelical axis is 20% of the contour length of the molecules) and then the third-order helical axis whose length is about 10% of the contour length of the relaxed molecule. In other words, a step-by-step folding of the DNA molecule in two and four, respectively, takes place. The compaction

process ends with the formation of minitoroids with a diameter of about 50 nm and semispheroids and spheroids. A low amount of visualized scDNA molecules with a superhelical axis length $l \sim 140$ nm (~3%) and semispheroids (~4%) as compared with the amount of spheroids (~17%) indicates, in our opinion, that both semispheroids and overscDNAs forming the third-order helical axis are intermediate (i.e., transient) forms in the compaction of scDNAs to spheroids.

It is known that the genomic DNA of *Escherichia coli* is localized in duplex nucleoids [7]. The degree of DNA compaction in nucleoids isolated in the presence of natural multivalent polyamines, such as polylysine, spermine⁴⁺, and spermidine³⁺ is similar to that of native nucleoids *in vivo* and substantially higher than in nucleoids isolated in the absence of polycations. The retention of the duplex nucleoid and the possibility to control DNA compaction in *E. coli* nucleoids by changing the polycation concentration indicate an important role of polycations in the compaction of genomic DNA *in vivo*.

It is interesting to note that the theoretical value of the diameter of DNA double helix (2 nm) significantly differs from the values of height (0.3–0.4 nm) and width (7–10 nm) of the molecule experimentally measured from AFM images. This is due to several reasons. It is commonly supposed that, in the measurement of the DNA strand width, the increase in the DNA diameter is due to a large radius of rounding of the AFM probe (5–10 nm), insufficient fixation of DNA molecules on support, etc. However, the reliable coincidence of the theoretically calculated excluded volume of the pGEMEX DNA and the volume of the DNA molecule determined from AFM images (see table) suggests that the increase in the DNA diameter upon adsorption onto mica is not due to instrumental errors. We think that the inconsistency of the measured width with the theoretically calculated diameter of DNA molecules is due to their conformational changes by the action of the surface properties of mica, which are accompanied by a considerable decrease in their height but, at the same time, with the retention of volume. We would like to particularly emphasize this circumstance, because the high values of the width of DNA molecules immobilized on mica is explained in the majority of studies of the AFM visualization of DNA [4, 28] just by an instrumental errors and insufficient fixation of biomolecules. Thus, our explanation for the increase in the DNA diameter under AFM measurements abolishes the available contradiction between the highest subnanometer resolution of AFM along the Z coordinate and the error in the lateral measurement of the DNA diameter.

Theoretical [39] and experimental [24, 40] studies of the amino mica surface revealed problems in the formation of aminosilane layers on the surface of amino

mica treated by APTES vapors. It was found [24] that, along with APTES layers, mobile APTES molecules not built into the layers are present on the mica surface. The condensation of DNA on amino mica was explained just by the presence of these mobile elements, which act as multivalent cations. A study of the effect of relative ambient humidity on the immobilization of linear DNA on amino mica obtained by treatment in vapors of undistilled APTES, which is a very important circumstance, showed that, at a low relative humidity, no DNA condensation occurs because of absence of mobile APTES molecules on the mica surface. These results agree with the results of our study and explain the formation of DNA aggregates on mica obtained using undistilled APTES, which is just characterized by a high relative humidity.

It should be also taken into account that the properties of chemical compounds at the liquid–solid (in this case, mica) interface and in solution substantially differ. In other words, the surface properties of substrate substantially affect the molecules occurring near the surface. For example, it is known that the ionization constant of terminal groups of different silane derivatives adsorbed on a mica surface (determined from titration curves) is by 3–6 pH units lower than that in solution [41, 42]. The p*K* value for APTES in solution is ~10 [43], whereas the p*K* for the amino groups of APTES upon immobilization on the mica surface is ~7.

We used the same procedure for the preparation of sample for the modified and standard amino mica, on which only plectonemic scDNA molecules were visualized and highly compacted structures were absent. This means that the compaction of DNA molecules occurs by the action of surface properties of modified amino mica. We think that the compaction of scDNA molecules in solution occurs near the amino mica surface, because, in this case, both the conformational mobility of molecules and a high level of shielding of the DNA phosphate groups necessary for compaction are provided.

EXPERIMENTAL

The following chemicals were used: HEPES, TE buffer of analytical grade, *N,N*-diisopropylethylamine of research grade, mica of technical grade, argon of technical grade (Wakenyaku, Japan); 3-aminopropyltriethoxysilane (APTES) of research grade (Aldrich); and pGEMEX1 DNA (Promega).

Preparation of DNA samples for AFM. pGEMEX1 scDNA of 3993 bp long was used without additional purification (Fig. 8). The presence of one band on the electrophoregram for the scDNA fraction (whose mobility in the gel is the same as that of 4000-bp marker) indicates the homogeneity of the sample throughout the length of the sequence.

Freshly cleaved mica, standard amino mica, and a modified amino mica were used as substrates. DNA was applied on a **freshly cleaved mica** using 10 mM HEPES buffer containing 2.5 mM MgCl₂ (note that Mg²⁺ ions are used only for immobilizing DNA on freshly cleaved mica). A drop of DNA solution in TE buffer (10 mM Tris-HCl, pH 7.9, 1 mM EDTA) (10 μl) without magnesium ions was applied on a strip of **amino mica or modified amino mica** of size 1 cm², the strip was rinsed after a 2-min exposure with deionized water, blown dry with a stream of argon, and the sample was kept for 20 min at a pressure of 100 mm Hg. For visualization of single molecules, the stock DNA solution at a concentration of 2 μg/ml was diluted with TE buffer to a concentration of 0.022 μg/ml to detect 7–10 molecules for an image of 2 × 2 μm and provide the frequency of compacted molecules acceptable for statistical processing.

Standard amino mica was prepared as described in [29] by the modification of freshly cleaved mica with amino groups in vapors of distilled APTES and *N,N*-diisopropylethylamine. The distillation of APTES was carried out at a reduced pressure in argon atmosphere. For amino modification, a freshly cleaved mica was incubated for 1 h with APTES and *N,N*-diisopropylethylamine solutions in a 2.5-l glass desiccator filled with argon. The modified mica was stored in the desiccator in an atmosphere of argon for one month. Buffer solutions and DNA samples were prepared using ultrapure water with a specific resistance of ~17 Mohm cm obtained on a Milli Q device (Millipore, United States).

Modified mica was obtained by minor modifications of the method used for the preparation of the standard amino mica [20]. In brief, the procedure was as follows. Freshly cleaved mica was modified using triple distilled APTES in a 2.5-l glass desiccator filled with argon. An APTES solution (120 μl) in the cover from a plastic micro test tube was placed for 4 h and *N,N*-diisopropylethylamine (40 μl), for 5 h to the bottom of the desiccator. The distillation of APTES was carried out at a reduced pressure in argon atmosphere. For the amino modification of mica, freshly cleaved mica was kept for 24 h in the desiccator in vapors of APTES and *N,N*-diisopropylethylamine. Both standard and modified amino mica were characterized using immobilized pGEMEX scDNA molecules on an area of 4 μm². The half-period of activity of standard amino mica was about 14 days; i.e., the amount of immobilized DNA molecules after the storage in argon atmosphere decreased two times. The half-period of activity of modified amino mica was about 28 days, which indicated that the amount of protonated amino groups was two times greater than in standard amino mica, i.e., the protonation of amino groups was about 100%.

Atomic force microscopy. A Nanoscope IV MultiMode System (Veeco Instruments Inc., United States) equipped with an E scanner (maximum range 12 μm) was used. AFM images of DNA were recorded at room temperature in air using a tapping variant of AFM in the "height" regime. Scanning was carried out by OMCL-AC160TS cantilevers (Olympus Optical Co., Japan), which have a resonance frequency of 340–360 kHz and a spring constant of 42 N/m. Scanning frequency was 3 Hz. Images were obtained at 512 \times 512 pixel format, smoothed, and analyzed using the Nanoscope software, version 5.12r3 (Veeco Instruments Inc., United States).

The volume of DNA molecules was calculated from the parameters of DNA molecules (height, length, and width) measured from AFM images. For a more precise determination of molecular volume, longitudinal, as a rule, and cross sections of molecules were constructed using the built-in option of the Nanoscope software.

ACKNOWLEDGMENTS

We thank O.Yu. Limanskaya (Institute of Microbiology and Immunology, Academy of Medical Sciences of Ukraine) and A.V. Shestopalova (Institute of Radiophysics and Electronics, National Academy of Sciences of Ukraine) for help and critical remarks during the preparation of the manuscript.

The study was partially supported by the Japanese Society for the Promotion of Science (Japan).

REFERENCES

- Kim, J., Yoshimura, S., Hizume, K., Ohniwa, R., Ishihama, A., and Takeyasu, K., *Nucleic Acids Res.*, 2004, vol. 32, pp. 1982–1992.
- Hizume, K., Yoshimura, S., Maruyama, H., Kim, J., Wada, H., and Takeyasu, K., *Arch. Histol. Cytol.*, 2002, vol. 65, pp. 405–413.
- Gonzalez-Huici, V., Salas, M., and Hermoso, J., *Nucleic Acids Res.*, 2004, vol. 32, pp. 2306–2314.
- Yoshimura, S., Hizume, K., Murakami, A., Sutani, T., Takeyasu, K., and Yanagida, M., *Curr. Biol.*, 2002, vol. 12, pp. 508–513.
- Morgan, J., Blankenship, J., and Mattheus, H., *Biochemistry*, 1987, vol. 26, pp. 3643–3649.
- Zinchenko, A. and Yoshikawa, K., *Biophys. J.*, 2005, vol. 88, pp. 4118–4123.
- Dame, R., Wyman, C., and Goosen, N., *Nucleic Acids Res.*, 2000, vol. 28, pp. 3504–3510.
- Kemura, K., Rybenkov, V., Crison, N., Hirano, T., and Cozzarelli, N., *Cell*, 1999, vol. 98, pp. 239–248.
- Sato, M., Ura, K., Hohmura, K., Tokumasu, F., Yoshimura, S., Hanaoka, F., and Takeyasu, K., *FEBS Lett.*, 1999, vol. 452, pp. 267–271.
- Martinkina, L., Klinov, D., Kolesnikov, A., Yurchenko, V., Streltsov, S., Neretina, T., Demin, V., and Vengerov, Y., *J. Biomol. Structure Dynamics*, 2000, vol. 17, pp. 687–695.
- Martinkina, L., Kolesnikov, A., Streltsov, S., Yurchenko, V., and Vengerov, Y., *J. Biomol. Structure Dynamics*, 1998, vol. 15, pp. 949–957.
- Golan, R., Pietrasanta, L., Hsieh, W., and Hansma, H., *Biochemistry*, 1999, vol. 38, pp. 14 069–14 076.
- Allen, M., Bradbary, E., and Balhorn, R., *Nucleic Acids Res.*, 1997, vol. 25, pp. 2221–2226.
- Dunlap, D., Maggi, A., Soria, M., and Monaco, L., *Nucleic Acids Res.*, 1997, vol. 25, pp. 3095–3101.
- Bloomfield, V., *Biopolymers*, 1997, vol. 44, pp. 269–282.
- Fang, Y. and Hoh, J., *Nucleic Acids Res.*, 1998, vol. 26, pp. 588–593.
- Cherny, D. and Jovin, T., *J. Mol. Biol.*, 2001, vol. 313, pp. 295–307.
- Hud, N. and Downing, K., *Proc. Natl. Acad. Sci. USA*, 2001, vol. 98, pp. 14 925–14 930.
- Lin, C., Wang, C., Feng, X., Liu, M., and Bai, C., *Nucleic Acids Res.*, 1998, vol. 26, pp. 3228–3234.
- Limanskii, A.P., Limanskaya, O.Yu., Volyanskii, A.Yu., Rudenko, S.S., Drach, M.I., and Limanskaya, L.A., Ukr. Patent no. 13571, Promyslova vlasnist., 2006, no. 4, p. 6.
- Butt, H., *Biophys. J.*, 1991, vol. 60, pp. 1438–1444.
- Bezanilla, M., Drake, B., Nudler, E., Kashlev, M., Hansma, P., and Hansma, H., *Biophys. J.*, 1994, vol. 67, pp. 2454–2459.
- Lyubchenko, Y. and Shlyakhtenko, L., *Proc. Natl. Acad. Sci. USA*, 1997, vol. 94, pp. 496–501.
- Fang, Y. and Hoh, J., *Nucleic Acids Res.*, 1998, vol. 26, pp. 588–593.
- Umemura, K., Ishikawa, M., and Kuroda, R., *Anal. Biochem.*, 2001, vol. 290, pp. 232–237.
- Limanskaya, O.Yu., Limanskaya, L.A., and Limanskii, A.P., *Biopolim. Kletka*, 2005, vol. 21, pp. 515–524.
- Limanskaya, O.Yu., Limanskaya, L.A., and Limanskii, A.P., *Biopolim. Kletka*, 2006, vol. 22, pp. 18–28.
- Shlyakhtenko, L., Gall, A., Weimer, J., Hawn, D., and Lyubchenko, Y., *Biophys. J.*, 1999, vol. 77, pp. 568–576.
- Manning, G., *Q. Rev. Biophys.*, 1978, vol. 11, pp. 179–2.
- Anderson, C. and Record, M., *Ann. Rev. Phys. Chem.*, 1995, vol. 46, pp. 657–7.
- Matulis, D., Rouzina, I., and Bloomfield, V., *J. Mol. Biol.*, 2000, vol. 296, pp. 1053–1063.
- Frank-Kamenetskii, M., Anshelevich, V., and Lukashin, A., *Usp. Fiz. Nauk*, 1987, vol. 151, pp. 595–618.
- Matulis, D., Rouzina, I., and Bloomfield, V., *J. Am. Chem. Soc.*, 2002, vol. 124, pp. 7331–7342.
- Korolev, N., Lyubartsev, A., Laaksonen, A., and Nordenkiold, L., *Nucleic Acids Res.*, 2003, vol. 31, pp. 5971–5981.
- Reiner, C., Stroh, C., Ebner, A., Klampfl, C., Gall, A., Romanin, C., Lyubchenko, Y., Hinterdorfer, P., and Gruber, H., *Anal. Chimica Acta*, 2003, vol. 479, pp. 59–75.

36. Limansky, A., Shlyakhtenko, L., Schaus, S., Henderson, E., and Lyubchenko, Y., *Probe Microscopy*, 2002, vol. 2, pp. 227–234.
37. Hansma, H., Golan, R., Hsieh, W., Lollo, C., Mullen-Ley, P., and Kwoh, D., *Nucleic Acids Res.*, 1998, vol. 26, pp. 2481–2487.
38. Boles, T., White, J., and Cozzarelli, N., *J. Mol. Biol.*, 1990, vol. 213, pp. 931–951.
39. Fujimoto, B. and Schurr, J., *Biophys. J.*, 2002, vol. 82, pp. 3286–3291.
40. Crampton, N., Bonass, W.A., Kirkham, J., and Thomson, N.H., *Langmuir*, 2005, vol. 21, pp. 7884–7891.
41. Vezenov, D., Noy, A., Rozsnyai, L., and Lieber, C., *J. Am. Chem. Soc.*, 1997, vol. 119, pp. 2006–2015.
42. Zhang, H., He, H., Wang, J., Mu, T., and Liu, Z., *Appl. Phys.*, 1998, vol. A66, pp. S269–S271.
43. Limanskii, A.P., *Biopolim. Kletka*, 2001, vol. 17, pp. 292–297.